Ullah *et al. Geoscience Letters* (2023) 10:53
https://doi.org/10.1186/s40562-023-00308-4

Geoscience Letters

RESEARCH LETTER

Open Access

Structures and stratigraphy of Al Jaww Plain, southeastern Al Ain, United Arab Emirates: implications for aquifer systems and mantle thrust sheet

Saif Ullah[1*], Mohammed Y. Ali[1], Muhammad A. Iqbal[1], Fateh Bouchaala[1] and Hakim Saibi[2]

Abstract

The United Arab Emirates (UAE) is dependent on desalinated water and shallow aquifers to satisfy its freshwater requirements. Despite the paramount importance of understanding the depth and spatial extent of these aquifers, comprehensive investigations into the properties of these aquifers, as well as the underlying subsurface structures and stratigraphy, have been conspicuously lacking. This study presents the findings of integrated geophysical and borehole investigations conducted in the Al Jaww Plain, southeastern Al Ain, UAE, focusing on the properties of groundwater aquifers, the Semail ophiolite contact, and subsurface structures and stratigraphy. Through the analysis of groundwater borehole data, three interconnected types of groundwater aquifers have been identified, and characterized by their hydrogeological properties. The near-surface Quaternary unconfined aquifer, with an average thickness of 25 m, represents a fresh groundwater aquifer. The second aquifer, with an average thickness of 110 m, is connected to the upper Quaternary freshwater aquifer and is interpreted as part of the surficial aquifer system. The third aquifer has an average thickness of 200 m. By employing electrical resistivity tomography, the depth of the water table and groundwater potential in the shallow unconfined Quaternary aquifer near Jabal Mundassa have been estimated, aligning with the properties observed in the unconfined Quaternary aquifer across the entire Al Jaww Plain as depicted in the groundwater borehole cross section. In addition, this study provides insights into subsurface structures and stratigraphic features, revealing the westward extension of the Hawasina thrust sheet within the plain. Gravity and magnetic data analyses in the southeastern region of the Al Jaww Plain delineate the extent of the Semail ophiolite. Notably, magnetic data reveals the presence of an NW–SE-oriented magnetic anomaly detached from the main ophiolite thrust, which corresponds to the interpretation of the Semail ophiolite contact with sedimentary carbonate rocks on the Bouguer gravity map.

Keywords Structure, Stratigraphy, Quaternary aquifer, Semail ophiolite, Al Jaww Plain, UAE

Introduction

Geophysical investigation techniques have been widely employed to characterize subsurface structures and stratigraphy for groundwater and hydrocarbon exploration, particularly in geologically complex regions (Abdelrazek 2020; Binley et al. 2015; Casallas-Moreno et al. 2021; Rabeh et al. 2019). The Oman–United Arab Emirates (UAE) mountains boast the world's largest and thickest ophiolite, known as the Semail ophiolite, which was

*Correspondence:
Saif Ullah
saif.ullah@ku.ac.ae; geosaifullah@gmail.com
[1] Present Address: Department of Earth Sciences, Khalifa University of Science and Technology, Abu Dhabi, UAE
[2] Department of Geosciences, United Arab Emirates University, Al Ain, UAE

obducted during the Late Cretaceous (Ali et al. 2020). The emplacement of the Semail ophiolite, along with the collision between the Arabian and Eurasian plates in the late Oligocene–Miocene, resulted in the formation of a complex fold and thrust belt on the western flank of the Oman–UAE mountains (Ali et al. 2020; Noweir 2000; Searle 1988).

Numerous geological and geophysical studies have been conducted in this region to comprehend the deformation style of this intricate fold and thrust belt (Abdelmaksoud et al. 2022; Ali et al. 2009, 2020, 2008; Cooper et al. 2014; Noweir 2000; Rabu et al. 1993; Searle 1988; Searle and Ali 2009; Styles et al. 2006; Woodward 1994). Al Ain City, situated in the eastern UAE, is part of the fold and thrust belt of the Oman–UAE mountains that experienced significant structural deformation between the Late Cretaceous and Neogene (Searle and Ali 2009). Within the vicinity of Al Ain City, Al Jaww Plain, and Jabal Hafit anticline represent prominent features, where limited geophysical investigations have been conducted to understand subsurface stratigraphy, structural styles, and groundwater characteristics. Al Jaww Plain is bordered by the Oman–UAE mountains on the eastern side and the Jabal Hafit anticline on the western side (Fig. 1). It plays a crucial role in groundwater extraction for Al Ain City and its surrounding areas (El-Mahmoudi et al. 2004).

The Quaternary aquifers serve as the primary source of groundwater in Al Ain City and its surrounding regions, including the Al Jaww Plain (Kress 2017), serving the purposes of irrigation and fulfilling other groundwater consumption needs. Woodward (1994) utilized seismic sections covering the Al Jaww Plain and other areas of Al Ain to delineate the major structural elements influencing the Quaternary aquifers. El-Mahmoudi et al. (2004); El-Mahmoudi (2007) employed electric resistivity imaging techniques to map the hydro-stratigraphic units of the Quaternary aquifers in Al Jaww Plain. Ali et al. (2008) conducted a geophysical investigation using gravity, magnetic, and seismic reflection in the plain, elucidating the deformation style and stratigraphy of the Upper Cretaceous to Cenozoic sequences, the occurrence of the Semail ophiolite in the eastern part, and the extension of the Hawasina complex in the northwest part of the plain. Bruno and Vesnaver (2021) focused their investigation on groundwater characterization within the Al Jaww Plain, primarily through the examination of a 6 km seismic reflection profile. They highlighted the imperative need for supplementary key parameters derived from petrophysical logs and electric resistivity data to enhance the hydrological characterization of the subsurface, particularly for the purposes of groundwater exploration. Abdelmaksoud et al. (2023) oriented their research efforts toward elucidating the basement morphology and tectonostratigraphic evolution of the fold-and-thrust belt. Their study included an interpretation of the Al Jaww thrust, situated on the eastern periphery of the plain, which intersects the Cenozoic sequence and culminates within the Upper Cretaceous sequence. These studies failed to determine the thickness, extent, and hydrological properties of both unconfined and confined aquifers within the Quaternary and Miocene formations situated amidst the Jabal Hafit and Oman–UAE mountains within Al Jaww Plain. Furthermore, these investigations did not provide a definitive cartographic representation of the subterranean interface delineating the contact between the Semail ophiolite and the sedimentary strata.

In this study, we employed integrated seismic reflection profiles and groundwater borehole data across Al Jaww Plain, as well as gravity, magnetic, and electrical resistivity tomography (ERT) data in the southeastern part near Jabal Mundassa (Fig. 1), to gain further insights into the structures and stratigraphy of the Al Jaww Plain. The study also aimed to determine the depths, thicknesses, and hydrological properties of the aquifers within the plain. Our findings revealed the orientation and nature of the contact between the ultramafic rocks of the Semail ophiolite and the carbonate rocks. Furthermore, magnetic data identified an NW–SE-oriented, thin (75–150 m) Semail ophiolite thrust detached from the main thrust sheet. In addition, the study observed the water table and various aquifers with distinct properties within the Al Jaww Plain.

Geological setting

The Oman–UAE mountains, situated on the northeastern margin of the Arabian Plate, were formed as a result of two distinct compressional events that occurred during the Late Cretaceous and Late Oligocene–Miocene (Fig. 2). The initial compressional event led to the emplacement of thrust sheets as the Neo-Tethys Ocean closed during the Late Cretaceous. These allochthonous thrust sheets include the Sumeini Group, which comprises carbonate sediments from the shelf edge and slope; the Hawasina thrust complex, composed of distal-slope and deep-sea Tethyan sediments; the Haybi complex, consisting of exotic limestone, volcanic, and sub-ophiolitic metamorphic rocks; and the Semail ophiolite, a thick slab of oceanic crust and upper mantle rocks (Ali et al. 2008; Noweir 2000; Searle 1988, 2007; Searle and Cox 1999).

The obduction of the Semail ophiolite and allochthonous thrust sheets in the northeastern Arabian margin resulted in the Oman–UAE mountains downward flexure of the underlying autochthonous Mesozoic shelf carbonates, giving rise to the Aruma foreland basin

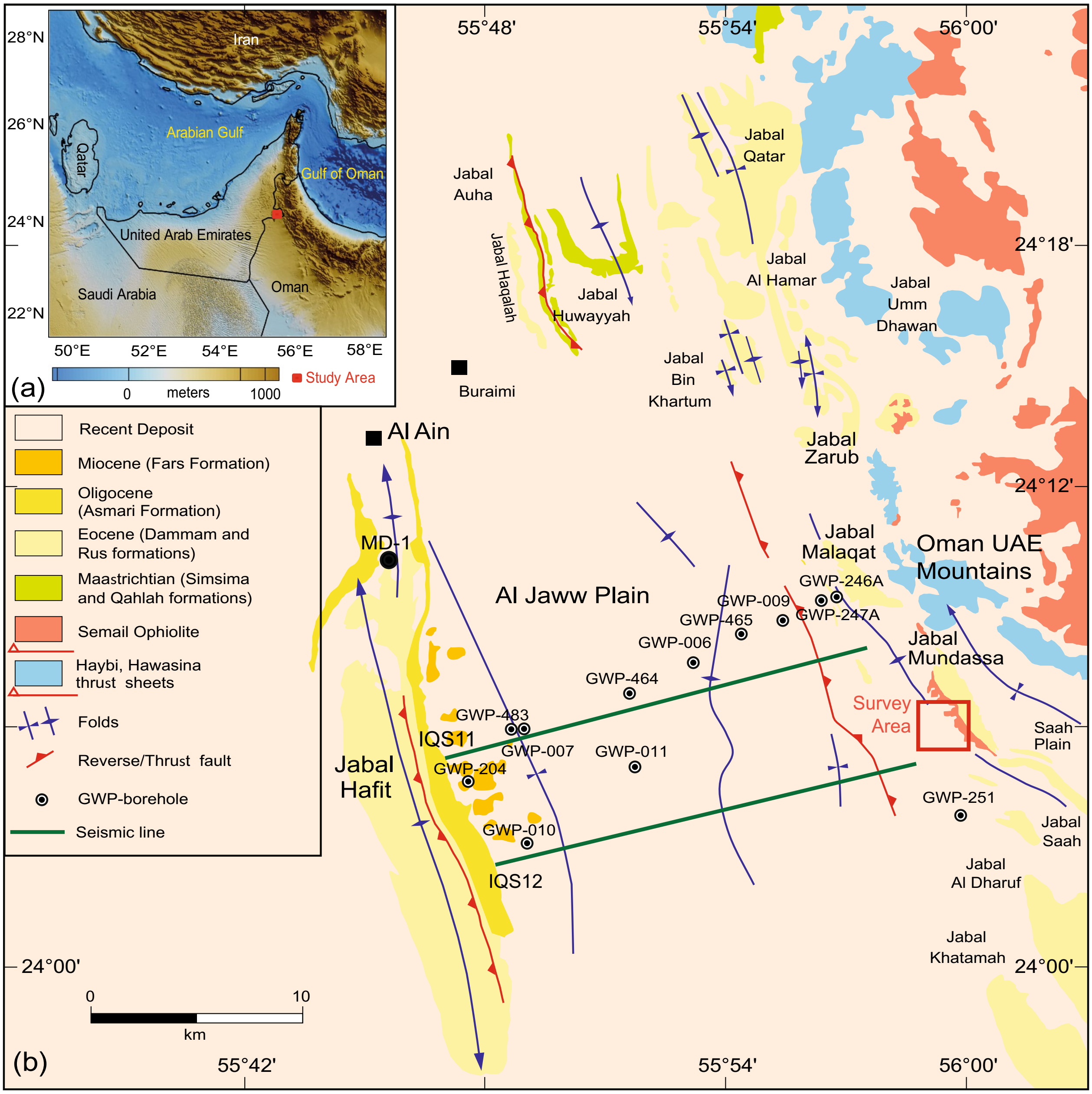

Fig. 1 **a** Topographic map of the United Arab Emirates (UAE) and surrounding region illustrating the study area (red box). **b** Geological map with subsurface structures of Al Jaww Plain and surrounding areas after Ali et al. (2008) showing the Location of the survey area. Locations of GWP boreholes and two seismic lines are also shown. MD-1 illustrates the location of the hydrocarbon exploration well used to depth convert the seismic profiles

and a flexural bulge on the western side of the UAE and Oman mountains. The obducted allochthonous units underwent significant deformation and caused regional uplift, leading to the partial erosion of the shelf carbonates of the Wasia Group. The Fiqa and Juwaiza formations subsequently filled the foreland basin during the Late Cretaceous, characterized mainly by mud, marl, and conglomerate lithologies. These foreland sequences are overlain by shallow-marine limestone of the Maastrichtian age, known as the Simsima Formation (Abd-Allah et al. 2013; Boote et al. 1990; Glennie 1974; Searle 1988; Warburton et al. 1990).

During the Late Oligocene–Miocene, a subsequent compressional event took place as a result of the

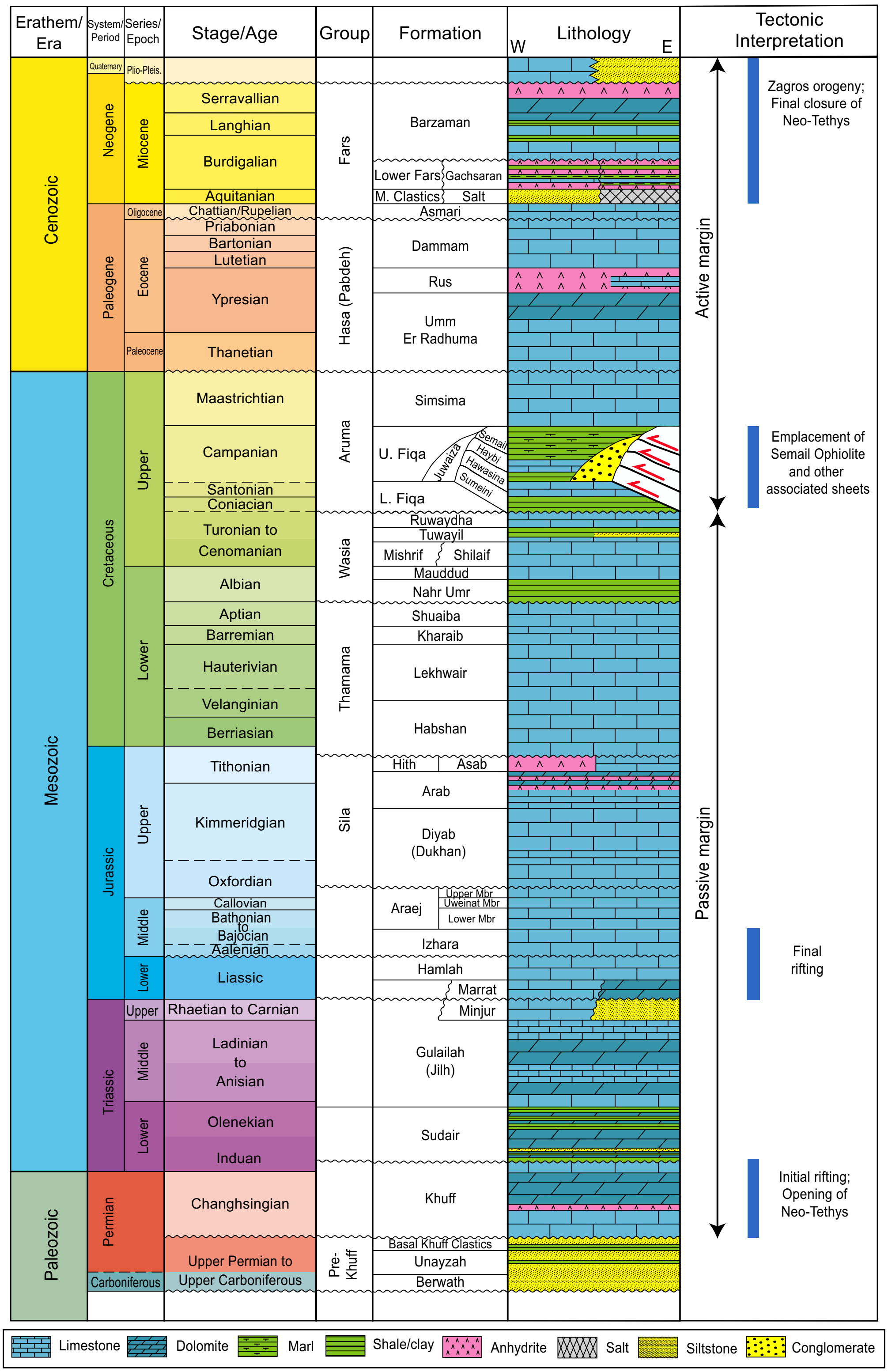

Fig. 2 Generalized tectono-stratigraphy of the northern Oman mountains showing the stratigraphic relationship of the Cenozoic and Upper Mesozoic groups (modified from Abdelmaksoud et al. 2022)

collision between the Arabian and Eurasian plates. This collision led to the formation of the Zagros fold and thrust belt on the Iranian side, the eastern fold and thrust belt in the Makran zone, and a complex fold and thrust belt adjacent to the Oman–UAE foreland basin. The collision also caused the uplift of sedimentary successions in the western part of the Oman–UAE mountains (Ali et al. 2008; Boote et al. 1990; Dunne et al. 1990; Searle et al. 1990). The uplifted sedimentary rocks underwent subsequent erosion, resulting in the removal of Neogene sequences. However, thick Upper Cretaceous and Cenozoic sections are still preserved in the eastern part of the UAE. Notable folded structures of Oligocene–Miocene age in the Al Ain region, trending in an NNW–SSE direction, include Jabal Hafit, Jabal Auha, Jabal Zarub, Jabal Malaqat, and Jabal Mundassa (Fig. 1).

The Al Jaww Plain is situated on the western foothills of the Oman–UAE mountains and lies on the southeastern side of Al Ain City. The exposed strata on the eastern side of the plain consist of the Upper Cretaceous to Lower Eocene age units of the Qahlah, Simsima, Umm Er Radhuma, Rus, and Dammam formations (Abd-Allah et al. 2013). The Qahlah and Simsima formations exhibit an unconformable contact with the Semail ophiolite and the folded thrust sheets of the Hawasina and Haybi complexes, which range from the Permian to Late Cretaceous in age (Glennie 1974; Wilson 2000) (Fig. 2). The Semail ophiolite primarily comprises serpentinite mantle rocks, which are predominantly exposed on the western side of the Jabal Malaqat and Jabal Mundassa outcrops. Within these outcrops, the Maastrichtian Simsima Formation is sandwiched between the serpentinite ophiolite at the bottom and the Umm Er Radhuma (Muthaymimah) Formation at the top. The upper and lower contacts of the Simsima Formation represent erosional surfaces and signify regional unconformities (Abd-Allah et al. 2013; Abdelghany 2003). On the summits of the Jabal Malaqat and Jabal Mundassa outcrops, the Eocene Rus and Dammam formations are exposed (Fig. 1). Jabal Hafit, located to the west of Al Jaww Plain, is a doubly plunging anticlinal structure, where Eocene-to-Miocene carbonate rocks are exposed. These rock units include the Dammam and Rus formations, the Oligocene Asmari Formation, and the Miocene Fars Formation (Abd-Allah et al. 2013; Searle and Ali 2009).

The Al Jaww Plain is bordered by Jabal Hafit to the west and Jabal Zarub, Jabal Malaqat, and Jabal Mundassa outcrop to the east, marking the border between the UAE and the Sultanate of Oman. It is a low-relief alluvial piedmont that slopes westward towards Jabal Hafit. The plain covers an area of approximately 550 km^2, with dimensions of 20 km wide in the east–west direction and 25 km long in the north–south direction (Ali et al. 2008; El-Mahmoudi et al. 2004; El-Mahmoudi 2007). The main subsurface structures in Al Jaww Plain trend almost parallel to Jabal Hafit (Ali et al. 2008; Woodward 1994).

The fillings of Al Jaww Plain primarily consist of Quaternary deposits derived from the surrounding mountains on the eastern side, transported into the plain through wadis (El-Mahmoudi 2007). During the rainy seasons, water channels originating from the eastern limb of the Jabal Hafit anticline also contribute to recharging the western part of the plain. The plain exhibits various types of near-surface sediments, including alluvial deposits, desert plain deposits, mixed deposits, sabkha deposits, and aeolian sands. These sediments are distributed in wadis with varying flow patterns and display complex braided channel morphologies (Menges et al. 1993). The alluvium in the plain consists of sand and gravel with interbeds of silt, marl, and clay at deeper levels. The coarse clastic units often contain a clay-rich matrix, typically calcareous (El-Mahmoudi et al. 2004; El-Mahmoudi 2007). The average thickness of the Quaternary alluvium deposits in Al Jaww Plain is around 30 m but can vary from 10 to 50 m due to subsurface structural conditions (Eggleston et al. 2020). Groundwater in the plain exhibits salinity ranging from fresh to slightly saline, with total dissolved solids (TDS) concentrations ranging from < 500 to 6500 mg/L (El-Mahmoudi 2007).

A specific area of approximately 3 km^2 was selected for high-resolution gravity, magnetic, and electrical resistivity tomography (ERT) investigations on the western edge of Jabal Mundassa in Al Jaww Plain. This survey area is located approximately 20 km east of Jabal Hafit, at the border between Oman and the UAE (Fig. 1). The surveyed area slopes southwest, and the exposed rocks on the eastern side comprise the Semail ophiolite, Simsima Formation, and Umm Er Radhuma Formation. The surface geology of the survey area consists of unconsolidated materials such as boulders, sand, and gravels eroded from nearby Jabal Mundassa and deposited here, along with small water channels originating from Jabal Mundassa. These water channels contribute to recharging the plain during rainy seasons.

Data and methodology

Groundwater well data

The Groundwater Research Program (GRP), conducted between 1988 and 2013 in the UAE, was a collaborative effort between the National Drilling Company and the US Geological Survey. Initially, the program focused on exploring the groundwater resources in the Abu Dhabi Emirate, but later transitioned into groundwater monitoring (Kress 2017). As part of this program, borehole data from eleven groundwater wells were collected and used to construct a geological cross section. The cross section extends from the southwest near Jabal Hafit to the northeast near Jabal Malaqat in Al Jaww Plain (Figs. 1 and 3). The cross section provides valuable insights into the geological formations and hydrogeological characteristics of the region, contributing to a better understanding of the groundwater resources in Al Jaww Plain.

Seismic profiles

The seismic profiles IQS11 and IQS12 were part of a comprehensive seismic survey conducted in the 1980s and 1990s for hydrocarbon exploration in the Al Ain area. These profiles were utilized to investigate the structure and stratigraphy of Al Jaww Plain (Figs. 1, 4, and 5). Each profile extends approximately 20 km and traverses across the Al Jaww Plain with a WSW–ENE orientation. The seismic data were recorded using Vibroseis as a seismic source, with a two-way-travel time (TWT) of up to 5 s and a sample interval of 4 ms.

In 2007, WesternGeco reprocessed both seismic profiles (Figs. 4 and 5) using standard seismic data processing techniques. The processing steps involved in the reprocessing included geometry assignment, field static corrections, trace editing, FK filtering to attenuate coherent noise, amplitude balancing, deconvolution filtering with an operator length of 160 ms, initial velocity analysis, pre-stack time migration, post-stack migration velocity analysis, and common mid-point stacking. By subjecting the seismic data to these processing sequences, the quality and clarity of the seismic profiles were enhanced, allowing for a more detailed analysis of the subsurface structures and stratigraphy of Al Jaww Plain.

The seismic profiles were depth-converted using velocity data obtained from velocity data of a nearby hydrocarbon exploration well MD-1 (Fig. 6), situated approximately 9 km from the commencement point of seismic profile IQS11 (Fig. 1) and the P-velocity tomographic inversion conducted by Bruno and Vesnaver (2021). In addition, we relied on lithological information and properties from the layers intersected by the groundwater borehole data to interpret the seismic profiles.

Gravity data

The survey area is delimited by the Jabal Mundassa outcrop on the eastern side and a road connecting to the Border Force Camp on the northwestern part (Figs. 1 and 7a). To analyze the gravity data in this area, a Digital Elevation Model (DEM) map was constructed using 30 m resolution SRTM (Shuttle Radar Topography Mission) data (Fig. 7b). The DEM map provides information about the elevation variations in the survey area, ranging from 390 m above mean sea level (amsl) to over 430 m amsl. The highest point is located at the top of the Jabal

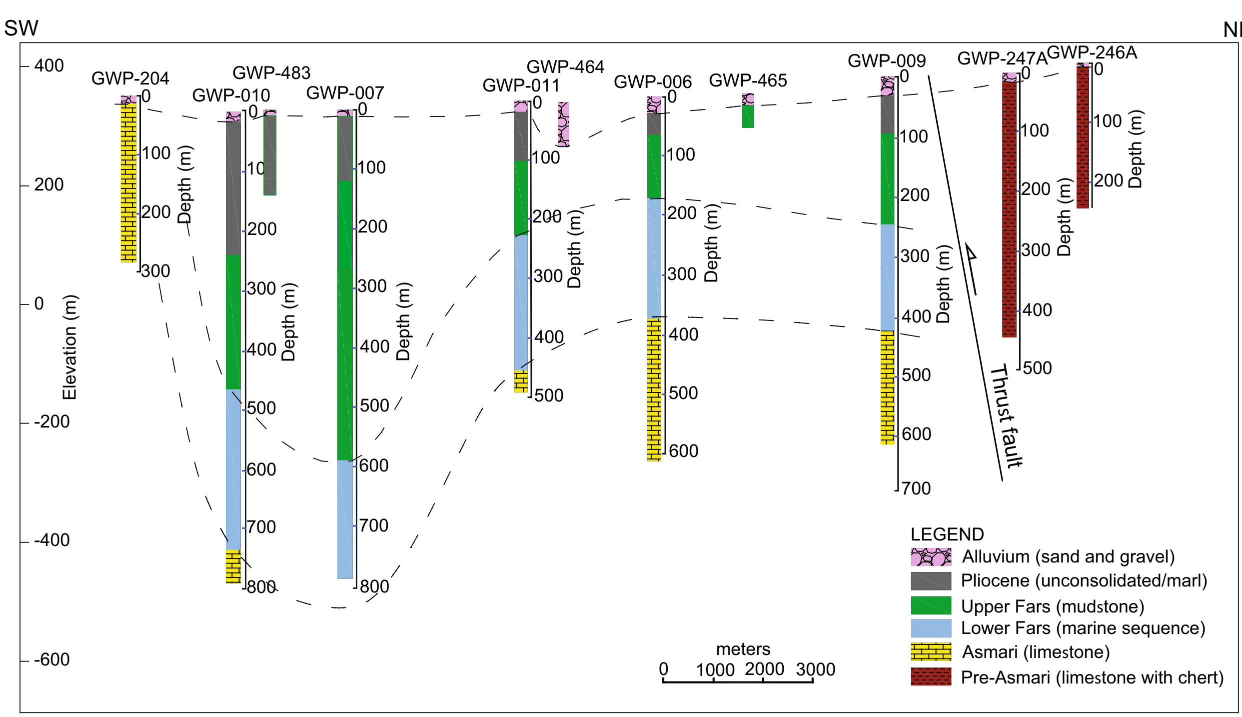

Fig. 3 GWP borehole cross section across Al Jaww Plain showing stratigraphy and thicknesses encountered by the boreholes

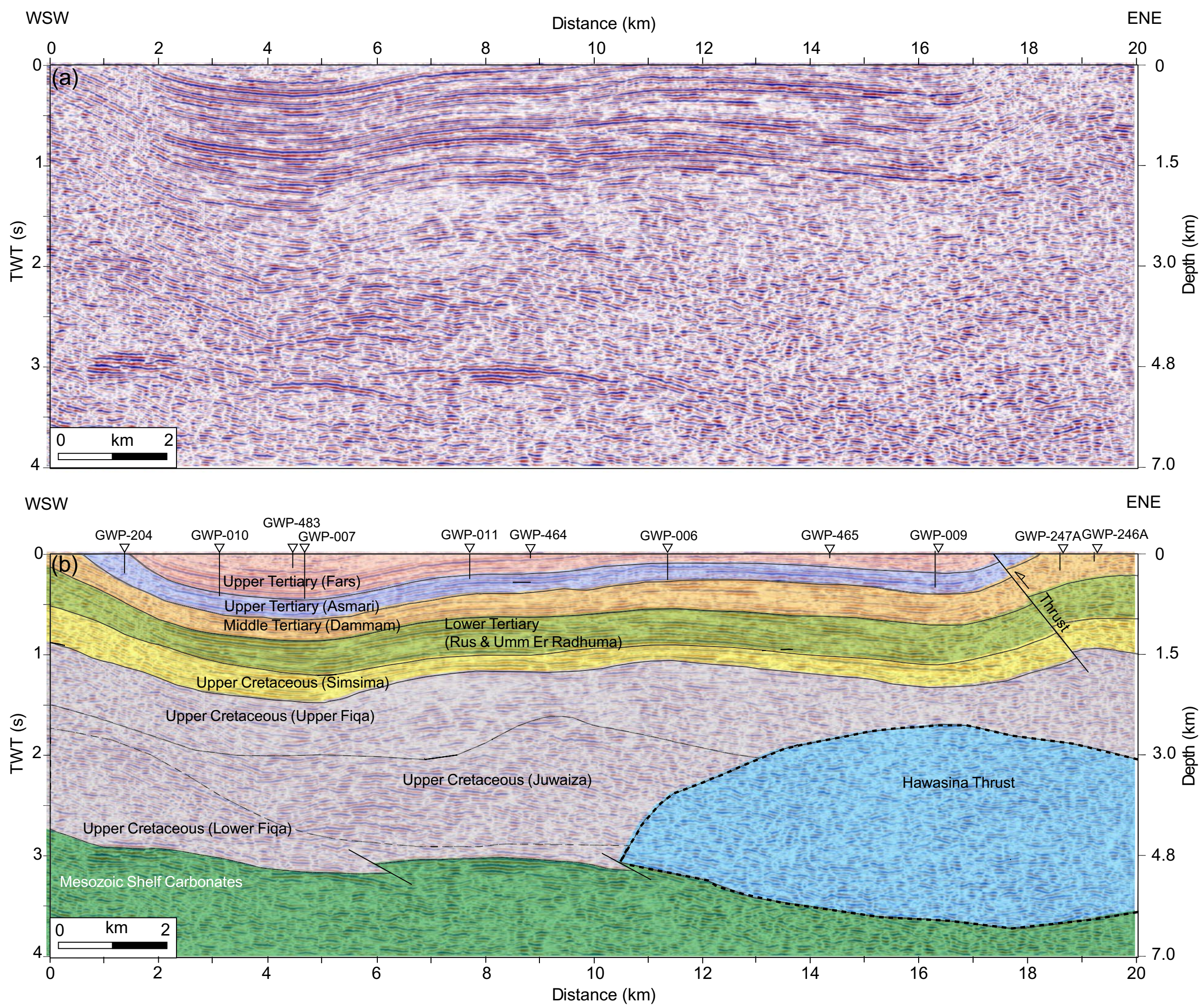

Fig. 4 **a** Un-interpreted seismic profile IQS11 across Al Jaww Plain (for location see Fig. 1). **b** Interpreted seismic profile IQS11 showing a series of folds and a high-angle thrust fault. The profile also illustrates the stratigraphic correlation of Cenozoic, Upper Cretaceous Simsima, Fiqa, Juwaiza, Hawasina thrust Allochthon, and Mesozoic shelf carbonates. The seismic profile was depth converted based on a velocity profile obtained from a nearby hydrocarbon exploration well MD-1 (Fig. 1) and the P-velocity tomographic inversion conducted by Bruno and Vesnaver (2021). TWT stands for two-way travel time

Mundassa structure, with an elevation exceeding 550 m amsl. The DEM map is utilized to calculate the terrain correction for the gravity data in this region.

A total of 911 gravity stations were acquired in the survey area using a Scintrex CG5 gravimeter (Fig. 8). Initially, a station interval of 200 m was selected to cover the entire survey area, but it was later reduced to fill in the gaps. The spacing between gravity stations ranges from approximately 30 to 100 m in the central part of the survey area. A base station was established at the southeastern corner of the survey area (Fig. 8a).

The processing workflow for the gravity data reduction included corrections for instrument drift, latitude, elevation, Bouguer, and terrain. The gravity data were then reduced to Bouguer anomaly using an average crustal density value of 2670 kg/m^3. The gravity data were tied to an absolute base station established by Ali et al. (2008) in Al Jaww Plain. Finally, terrain correction was applied within a local correction distance of 1.5 km, which accounts for the gravitational effects caused by the varying topography in the surrounding gravity survey area. Terrain correction corrects for irregularities in gravity measurements due to the terrain variations (Kane 1962; Nagy 1966).

The processed gravity data yielded a Bouguer anomaly map, which was then used to generate the regional

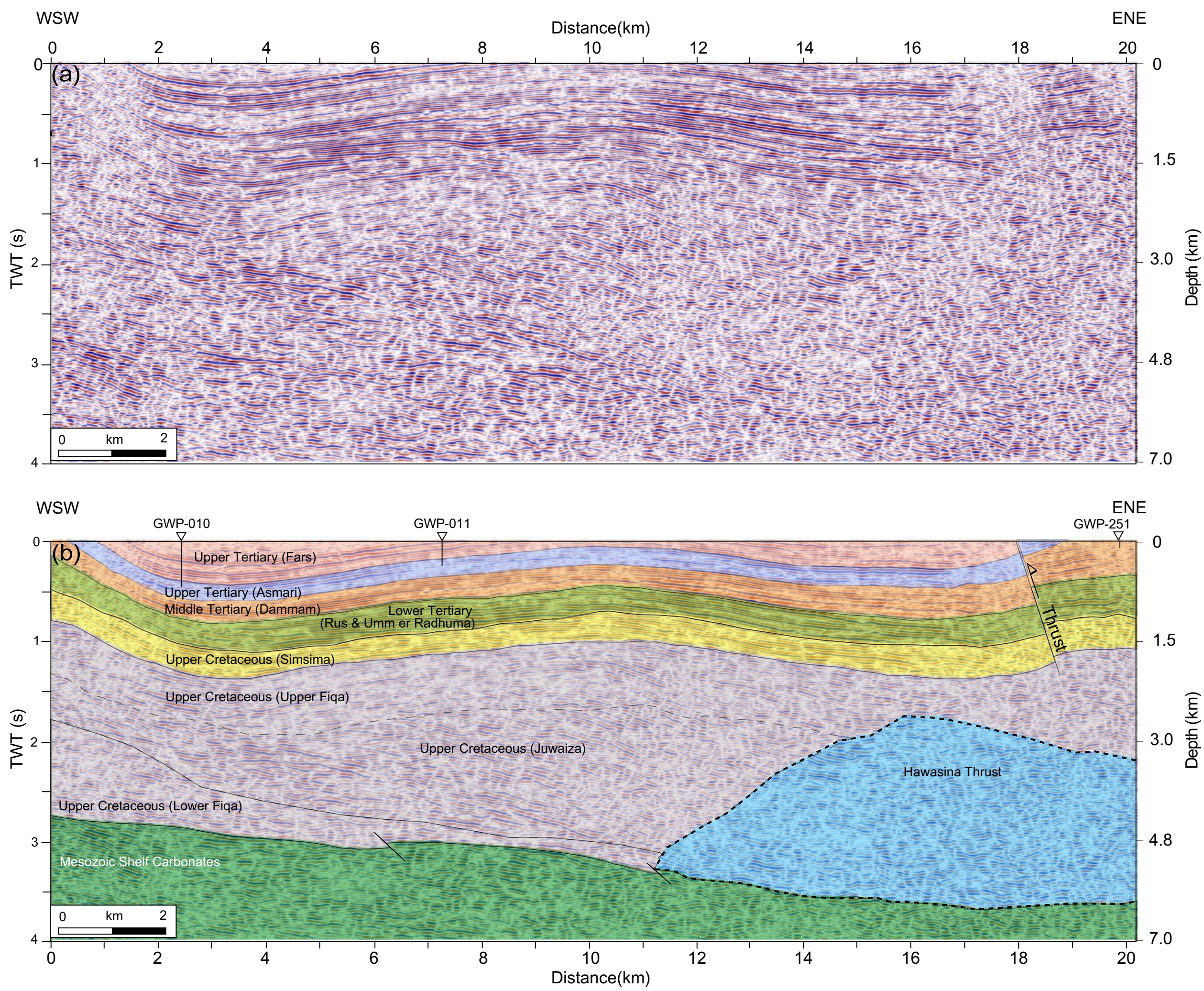

Fig. 5 **a** Un-interpreted seismic profile IQS12 across Al Jaww Plain (for location see Fig. 1). **b** Interpreted seismic profile IQS12 showing a series of folds and a high-angle thrust fault. The seismic profile was depth converted based on a velocity profile obtained from a nearby hydrocarbon exploration well MD-1 (Fig. 1) and the P-velocity tomographic inversion conducted by Bruno and Vesnaver (2021)

Bouguer anomaly at an elevation of 200 m using an upward continuation filtering technique (Fig. 8b). The residual Bouguer anomaly map (Fig. 8c) was obtained by subtracting the regional Bouguer anomaly (Fig. 8b) from the Bouguer anomaly grid (Fig. 8a).

Magnetic data

The magnetic data in the survey area were collected continuously at a 1-s time interval using two Geometrics G-858 magnetometers (Fig. 9). One of the magnetometers served as a base station to monitor diurnal variations resulting from magnetic storms during the survey period, while the other magnetometer with two sensors was used to acquire the data. Prior to each magnetic survey, both magnetometers' time was synchronized. Initially, a line interval of 200 m was planned to cover the survey grid in both the north-to-south and east-to-west directions. However, to fill in the gaps within the survey grid, a 100 m interval was utilized in both directions. Additional data were acquired on the middle eastern side of the survey area to determine the precise location of an anomaly observed in the area.

The processing of the magnetic data involved a diurnal correction to eliminate the influence of short-term variations caused by daily changes in the geomagnetic field. Subsequently, the magnetic data were gridded using the minimum curvature gridding method to generate a map of the total magnetic intensity (TMI). Finally, the International Geomagnetic Reference Field

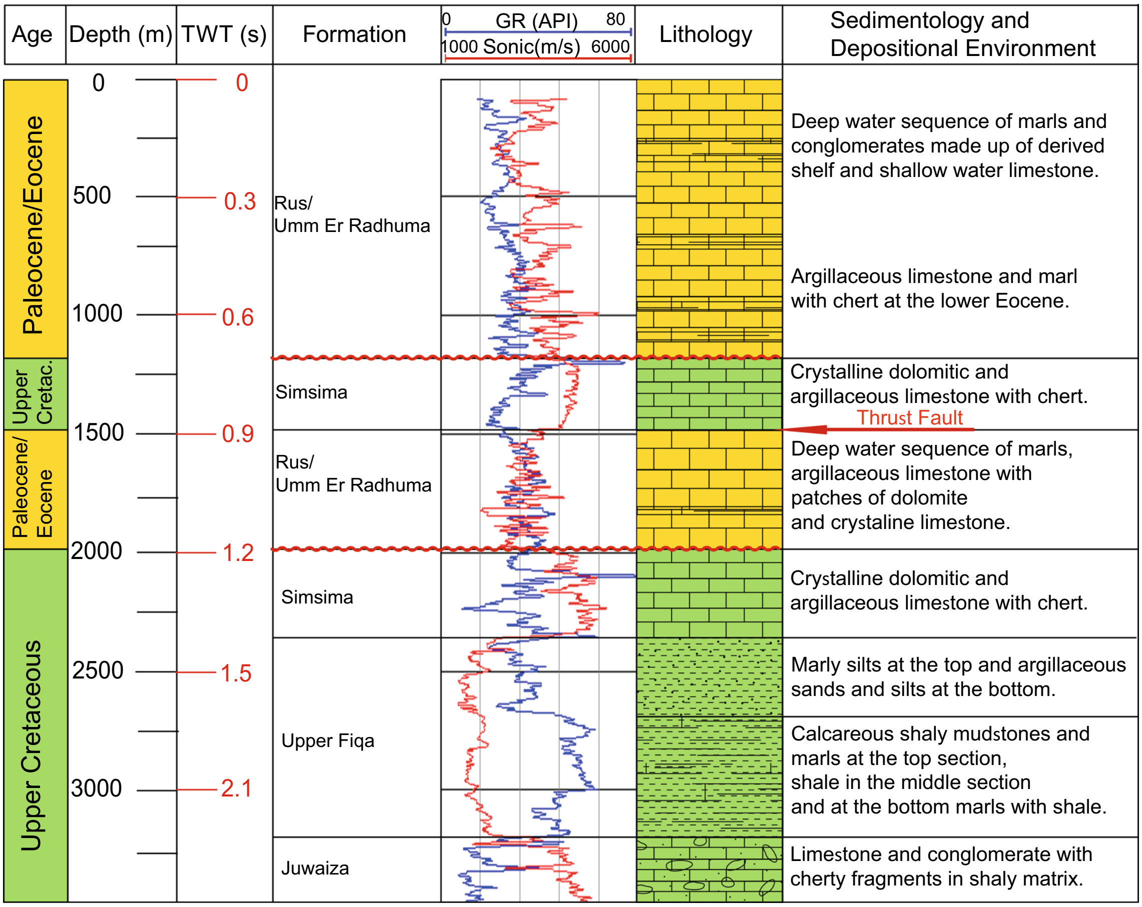

Fig. 6 Stratigraphy and petrophysical logs of the hydrocarbon exploration well MD-1 drilled approximately 9 km from the commencement point of seismic profile IQS11 (Fig. 1)

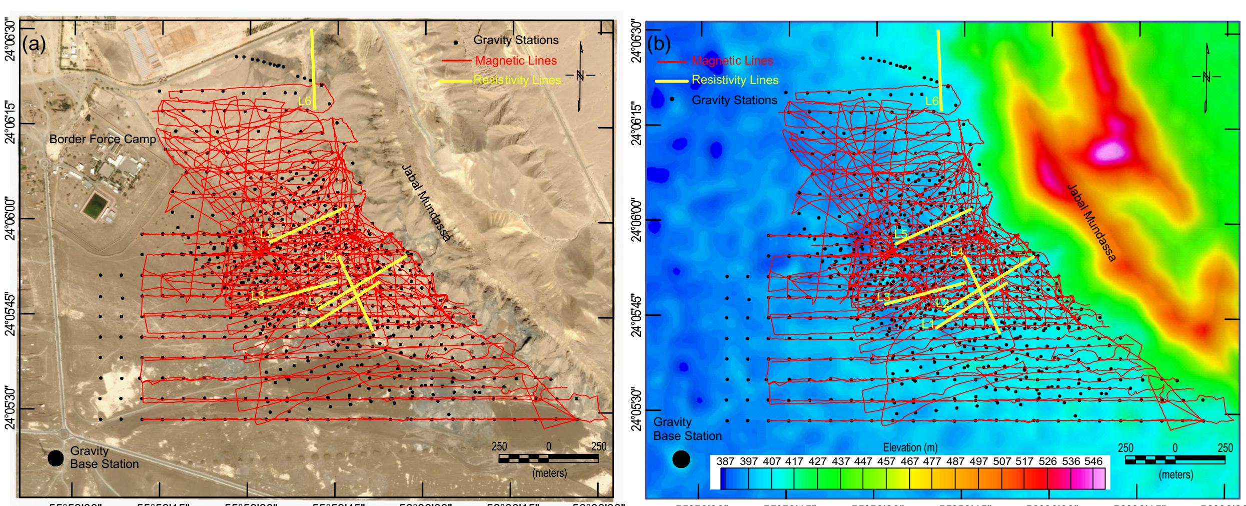

Fig. 7 **a** Satellite map of the survey area near Jabal Mundassa in Al Jaww Plain showing the location of gravity, magnetic, and resistivity stations. **b** SRTM Digital Elevation Model (DEM) map of a survey area near Jabal Mundassa in Al Jaww Plain showing locations of the gravity, magnetic, and electrical resistivity stations

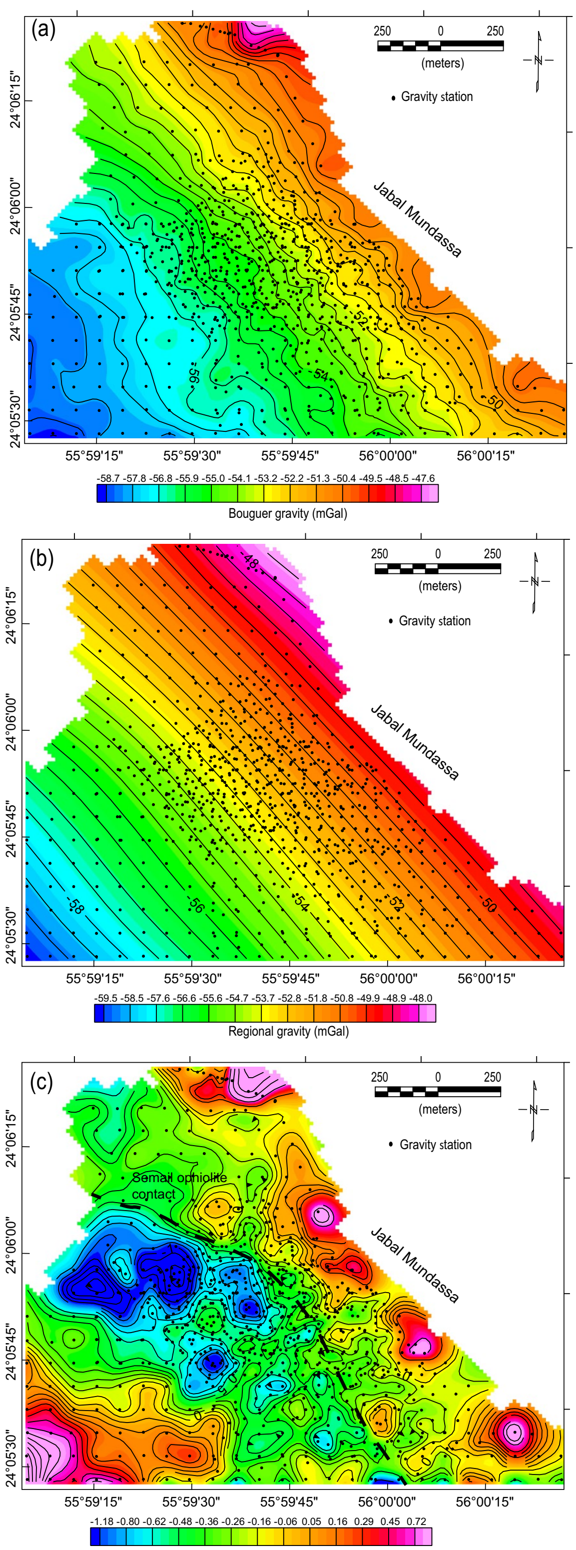

Fig. 8 **a** Bouguer anomaly map of the survey area near Jabal Mundassa. **b** Regional Bouguer anomaly map of the survey area near Jabal Mundassa. **c** Residual Bouguer Anomaly map of the survey area. The black dashed line shows the interpreted contact of the Semail ophiolite and sediments

and reduction to the pole (RTP) were applied to the TMI data. The RTP filter was applied to remove the effect of the magnetic inclination. The RTP operation transforms a magnetic anomaly caused by a source into an anomaly that would be produced by the same source if it were located at the pole and magnetized solely by an induced magnetization (Luo et al. 2010).

Electrical resistivity tomography data

The ERT data in the survey area were collected using an ABEM Terrameter LS instrument. Six ERT lines were established with varying lengths and orientations (Figs. 7 and 10). Each ERT line except for line 2 had a length of 400 m, while line 2 had a total length of 480 m. The data acquisition for each line involved the use of four resistivity-imaging cables, with each cable containing 21 take-outs and an electrode spacing of 5 m.

To differentiate the subsurface imaging results in the survey area, different electrode configurations were employed along the survey lines. It is worth noting that all the lines were approximately close to each other, contributing to a comprehensive understanding of the subsurface resistivity distribution. The specific data acquisition geometry and parameters for the ERT lines can be found in Table 1.

In the processing of the ERT data, the first step involved the removal of noisy data points from each ERT line. The noisy values, characterized by negative and very high resistivity, were attributed to high contact resistance at certain electrode locations. Despite using salty water to reduce contact resistance, some electrodes still exhibited noisy data due to the challenging surface geology comprising dry gravel and sand materials.

After editing each ERT data set to remove the noisy values, the apparent resistivity values were inverted to obtain the true resistivity values along the survey lines. Considering the dry surface conditions, a higher initial damping factor was applied. The inversion process consisted of seven iterations, with the Jacobian matrix updated after each iteration. The inversion was performed using a finite-element method with a robust data constraint, ensuring accurate determination of the subsurface resistivity distribution (Loke 2004). To solve the least square equation in the inversion process, the

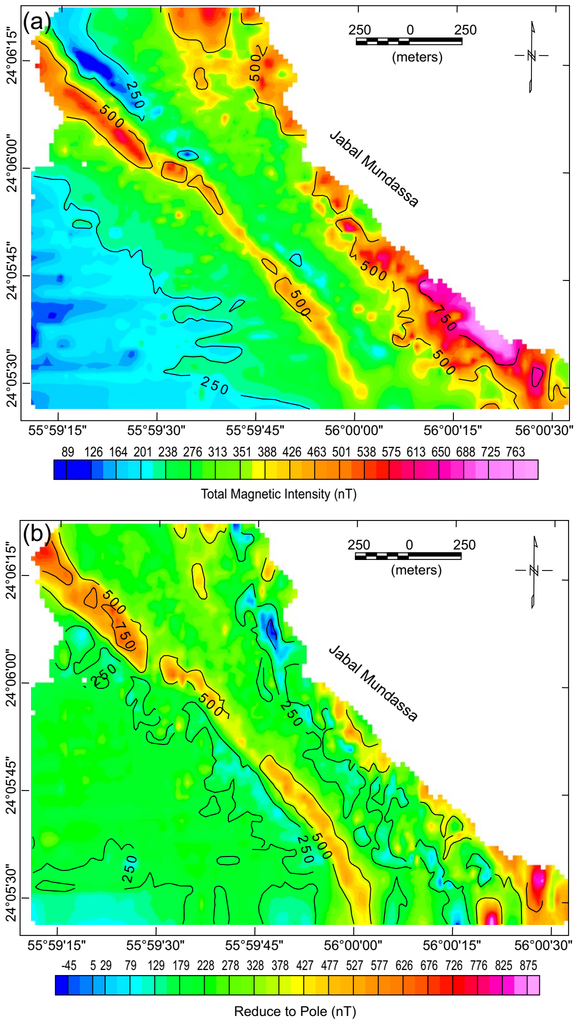

Fig. 9 **a** TMI (total magnetic intensity) map of the survey area. An NW–SE high anomaly is observed in the middle of the map. **b** RTP (reduction to the pole) map of the survey showing the NW–SE feature.

incomplete Gauss–Newton method was utilized. This approach enables the estimation of the true resistivity values by iteratively updating the model parameters to minimize the difference between observed and predicted apparent resistivity values (Loke 2004; Loke and Dahlin 2002).

Results

Groundwater boreholes cross section

The borehole cross section (Fig. 3) provides a comprehensive representation of the near-surface geology, hydro-stratigraphy, and lithological characteristics. It reveals the presence of Quaternary alluvium deposits consisting of sand and gravel, with thickness varying approximately between 10 and 75 m in the boreholes. Borehole GWP-464 exhibits the highest thickness of 75 m, while borehole GWP-246A demonstrates the lowest thickness of approximately 10 m.

Beneath the Quaternary alluvium lie the post-Fars Formation unit of the Pliocene age, consisting of poorly consolidated sand, gravel, and clay. The thickness of this unit varies among the boreholes and is more pronounced in the southwestern part of the cross section, coinciding with the formation of a syncline fold. The Miocene Upper Fars Formation, characterized by mudstone, slightly marl, and limestone rocks, is situated below the Pliocene deposits. The thickness of this unit varies along the cross section, with lesser thickness observed in the northeast and greater thickness in the southwest, particularly in the syncline structural position. Notably, borehole GWP-007 records a remarkable thickness exceeding 400 m for the Upper Fars Formation. The Lower Fars Formation comprises marine sequences, including interbedded shales, mudstones, and evaporate rocks. It is encountered at depths exceeding 200 m, particularly in the southwestern part of the cross section near Jabal Hafit, as evidenced by borehole GWP-010.

The Oligocene Asmari Formation consists of mainly limestone rocks. This formation occurs at a shallow depth immediately following the alluvium section on the southwest side, near the eastern edge of the Jabal Hafit anticline. In the middle portion of Al Jaww Plain, boreholes GPW-006 and GPW-009 reveal the Asmari Formation at greater depths.

In the eastern part of the Al Jaww Plain, near Jabal Malaqat, the cross section illustrates the presence of pre-Asmari limestone rocks with chert derived from the Eocene Rus and Dammam formations. These formations are thrusted and are observed in boreholes GWP-246A and GWP-247A towards the end of the cross section (Fig. 3). The borehole cross section provides valuable insights into the geological composition and structural characteristics of the subsurface, playing a crucial role in understanding the hydrogeological framework and groundwater resources of the region.

Seismic reflection profiles IQS11 and IQS12

The interpretation of seismic profiles IQS11 and IQS12 (Figs. 4 and 5) relies on the lithology and properties of the layers encountered by the adjacent hydrocarbon exploration well MD-1 (Fig. 6) and the shallow groundwater boreholes (Fig. 3). The seismic profiles provide insights into the near-surface geological structures, exhibiting continuous reflectivity sequences and distinct geometrical features. However, the bottom area and eastern side of both seismic profiles exhibit lower resolution and

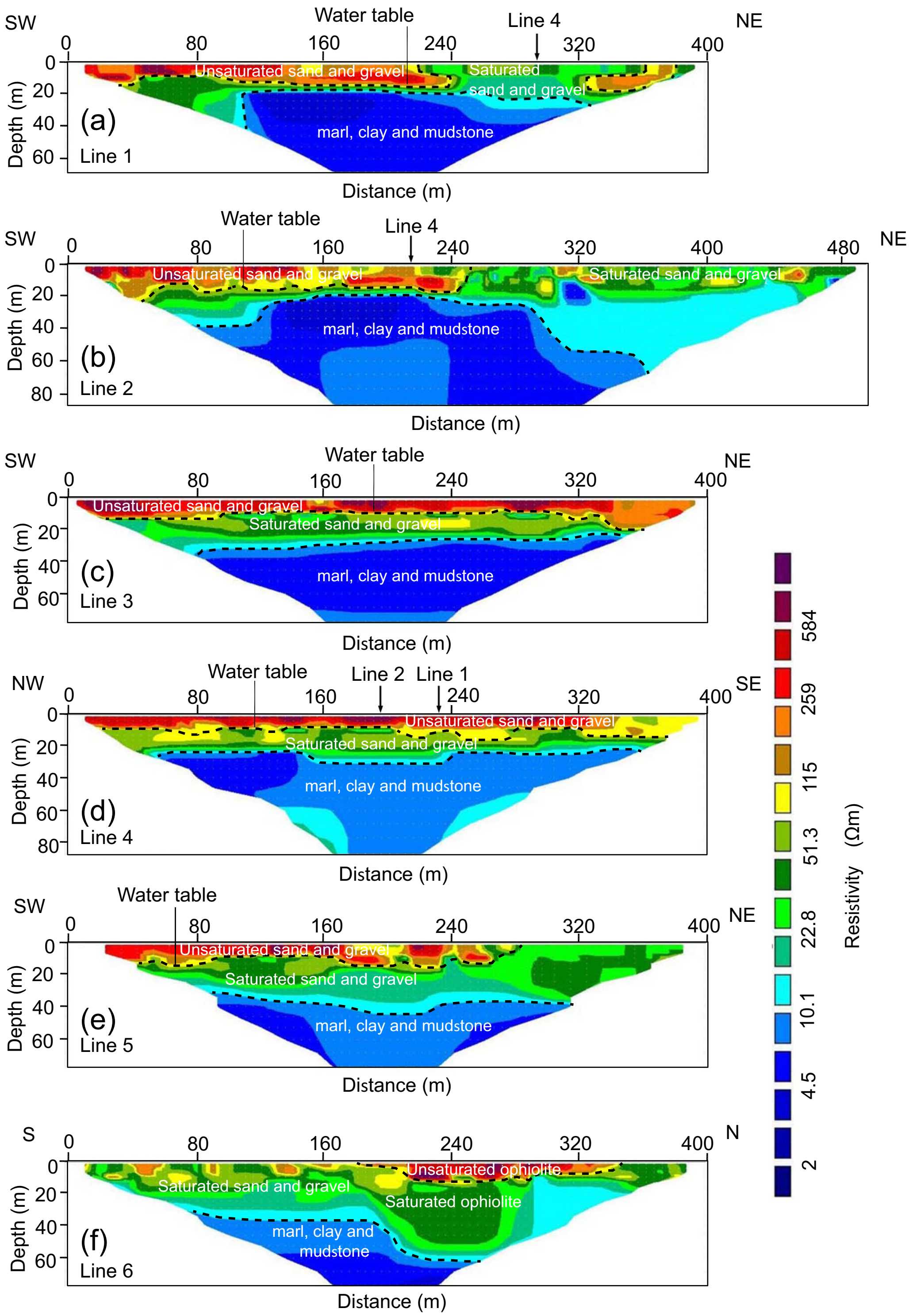

Fig. 10 ERT inverted sections of resistivity lines showing the interpretation of near-surface hydro-stratigraphic layers on the basis of groundwater borehole (GWP-251) results. **a** Line 1, **b** Line 2, **c** Line 3, **d** Line 4, **e** Line 5, and, **f** Line 6

Table 1 Acquisition geometry and parameters used for the ERT data

Line No	Electrode array	Electrode spacing (m)	Total length (m)	Total depth (m)	Line orientation
1	Wenner	5	400	65	SW–NE
2	Dipole–Dipole	5	480	85	SW–NE
3	Schlumberger	5	400	80	SW–NE
4	Dipole–Dipole	5	400	85	NW–SE
5	GradientPlus	5	400	75	SW–NE
6	GradientPlus	5	400	75	S–N

more complex seismic features compared to other parts of the profiles.

The interpretation of stratigraphic and tectonic features is primarily based on the seismic characteristics and reflection patterns, including the presence of prominent reflectors, reflector terminations, continuity, and amplitude. Existing publications in the area, such as Woodward (1994); Ali et al. (2008); Searle and Ali (2009); Ali et al. (2009); Cooper et al. (2014) and Bruno and Vesnaver (2021), have been utilized as references for the interpretation of the two seismic profiles.

The overall interpretation of the two seismic profiles reveals the presence of three distinct zones. The upper part corresponds to the Upper Cretaceous Simsima Formation and Cenozoic sequences. The middle part represents the Aruma foreland basin sequence and allochthonous thrust sheets. Finally, the lower part is interpreted as autochthonous Mesozoic shelf carbonates belonging to the Wasia and Thamama groups.

Gravity data

The gravity data obtained from the survey area in the southeastern part of Al Jaww Plain reveals distinct patterns in the Bouguer anomaly values. Near Jabal Mundassa, the region exhibits high-frequency Bouguer anomaly values, surpassing − 52 mGal. Conversely, the southwest side of the area displays low-frequency anomaly values, measuring less than − 57 mGal (Fig. 8a). Furthermore, a significant Bouguer anomaly feature with values exceeding − 48 mGal is observed to the north of the survey area, which can be attributed to the surface exposure of Semail ophiolite rock, as confirmed during the field survey.

The Bouguer anomaly values exhibit a smooth variation from the southwest to the northeast direction, with an average value of − 55 mGal observed in the central region of the map. The regional Bouguer anomaly map (Fig. 8b) presents a gradual change in values, ranging from − 59 mGal to − 47 mGal, along the southwest to northeast axis. This map is generated using the upward continuation filter technique, considering the limited extent of the survey area, with an upward continuation distance of 200 m. The residual Bouguer anomaly map (Fig. 8c) displays anomalies characterized by shorter wavelengths and higher frequencies. These anomalies can be attributed to the density variations in different near-surface materials within the survey area. The magnitude of the residual Bouguer anomaly ranges from − 0.95 mGal to 0.95 mGal, indicating the presence of localized density variations in the study region.

Magnetic data

The TMI map of the survey area reveals a distinct spatial pattern, with variations in magnetic field strength ranging from lower values (< 89 nT) to higher values (> 763 nT) in the southeast to the northeast direction (Fig. 9a). Notably, a prominent linear NW–SE feature exhibiting high TMI values (> 500 nT) is observed in the central region of the map. This feature follows a northwest-to-southeast trend and exhibits a slight inclination on the upper part. Importantly, it runs parallel to Jabal Mundassa, which is a prominent geological feature of the Oman–UAE mountains.

The RTP map provides further insights into the magnetic variations within the survey area (Fig. 9b). The NW–SE-oriented anomaly observed in the TMI map is more pronounced in the RTP map, particularly at the 500 nT and 750 nT contour levels. In addition, the tilt effect observed on the northwest side in the TMI map is removed in the RTP map, presenting a clearer representation of the magnetic anomalies in the region.

Electrical resistivity tomography (ERT) data

The results of the ERT inversion provide valuable insights into the hydro-stratigraphic properties of the near-surface Quaternary aquifer within the surveyed area (Fig. 10). The inverted ERT sections exhibit lateral and vertical variations in true resistivity across three distinct layers. In the near-surface layer, the first layer displays high resistivity values exceeding 115 Ωm. The second layer, located below the first layer, exhibits comparatively lower resistivity ranging from 15 to 115 Ωm.

Finally, the third layer, situated at the bottom of all ERT sections, demonstrates low resistivity values of less than 10 Ωm.

The total depth of all ERT sections is approximately uniform, reaching a depth of around 80 m, with the exception of Line 1, which has a depth of 70 m. Moreover, the inverted sections indicate that the water table varies between 10 and 15 m from the surface across all ERT sections (Fig. 10).

Discussion

Stratigraphy of Al Jaww Plain

The stratigraphy of the seismic profiles can be categorized into three primary sections: the lower, middle, and upper sections. The lower section is interpreted as autochthonous rocks composed of Mesozoic shelf carbonates, specifically the Wasia and Thamama groups. The Wasia Group, belonging to the middle Cretaceous, displays thrust faults at the boundary between the shelf carbonates and the Lower Fiqa Formation, which exhibits an unconformable contact (Figs. 4b and 5b).

The middle section is further divided into two parts: the Aruma foreland basin sequence and the allochthonous Hawasina thrust sheet. The Aruma foreland basin sequence comprises the Upper Cretaceous Fiqa and Juwaiza formations. Among these formations, the Fiqa Formation is the thickest, varying in thickness along the profiles. It can be further subdivided into Upper and Lower Fiqa formations. The Upper Fiqa Formation exhibits a continuous reflector sequence on the top, characterized by medium to high reflection features. However, the lower part of the formation shows complex seismic features. Varying configurations of high to low frequency, high amplitude, and internal reflectivity, ranging from parallel to sigmoid features are observed between the Lower and Upper Fiqa formations on the central-eastern part of the profiles. These features are interpreted as sandstone and conglomerate of the Juwaiza Formation (Figs. 4b and 5b). The Juwaiza Formation thins out on the eastern side of both seismic profiles. The Juwaiza Formation appears to be thinner in seismic profile IQS11 compared to IQS12. The Fiqa Formation represents the deposition of eroded material from allochthonous rocks, including the Hawasina-Hayabi thrust sheets and the Semail ophiolite. It primarily consists of marls, calcareous shales, and inter-bedded argillaceous limestone (Abd-Allah et al. 2013). The Qahlah Formation, a thin layer measuring 1–3 m, is exposed at Jabal Mundassa and Jabal Malaqat; hence, it is not interpreted in the seismic profiles.

In the eastern-central part of both seismic profiles, the seismic signals exhibit a composite nature and chaotic patterns, indicating the presence of a distinct rock unit. This rock unit is interpreted as the Hawasina thrust, which is part of the allochthonous rock sequence in this region. The Hawasina thrust demonstrates an unconformable contact with the surrounding rock units in both seismic profiles (Figs. 4 and 5). At the base, the Hawasina thrust exhibits an unconformable contact with the Lower Fiqa Formation, while it shows a similar contact with the Simsima Formation at the top, as observed in the end portions of both seismic profiles. The western edge of the Hawasina thrust sheet exhibits non-uniform characteristics in terms of seismic signals and is interpreted as pinching down at the base of the Juwaiza Formation.

The uppermost section in both seismic profiles corresponds to the Upper Cretaceous Simsima Formation and subsequent Cenozoic sequences. The seismic characteristics of this upper section exhibit pronounced reflection continuity, high frequencies, and strong amplitudes. The reflector sequences display parallel patterns and allow for differentiation of the Cenozoic sequences. The Simsima Formation, considered the basal unit of the Aruma Group, is confirmed to have contact with the underlying Fiqa Formation. Towards the southeastern side, the lower contact of the Simsima Formation is observed to be unconformable with the Hawasina thrust sheet (Figs. 4b and 5b). In the shallower parts of both seismic profiles, the stratigraphic units are interpreted to represent the Cenozoic sequences, owing to well-defined seismic sequence boundaries. The Cenozoic stratigraphic units identified include the Paleocene Umm Er Radhuma Formation and Eocene Rus and Dammam formations, the Oligocene Asmari Formation, and the Miocene Fars Group (Figs. 4b and 5b). The lithological characteristics of the Neogene units, such as the Asmari and Fars formations, align well with the data obtained from boreholes (Fig. 3).

Structures in Al Jaww Plain

The seismic profiles (Figs. 4b and 5b) exhibit various fold and thrust fault structures within Al Jaww Plain. Starting from the southwest side of the seismic profiles and progressing towards the northeast, a syncline fold is evident in the Cenozoic sequences, extending up to the Upper Cretaceous Fiqa Formation. The axis of this syncline fold is approximately 6 km east of the Jabal Hafit anticline structure. In the middle of the seismic profiles, an anticline structure with gentle slopes on both sides can be observed, corroborating the findings of the shallow borehole cross section (Fig. 3). This anticline leads to another syncline fold, characterized by a significant thrust fault on the eastern limb of the syncline. The thrust fault exhibits an eastward dip on both seismic profiles (Figs. 4b and 5b) and is also evident in the borehole cross section (Fig. 3). However, the dip angle of the thrust fault is steeper in profile IQS12 compared to the IQS11 profile. Moreover, towards the end of both seismic profiles, thrusting resulted in the erosion of the Miocene Fars Formation near the Oman–UAE mountains. The orientation of anticlines and synclines in both seismic profiles and shallow borehole cross section within Al Jaww Plain parallels the axis of exposed Jabal Hafit, Jabal Mundassa, and Jabal Malaqat. This axis exhibits a north–northwest-to-south–southeast direction. The subsurface structures and stratigraphy interpreted from the seismic profiles closely align with previous studies conducted in Al Jaww Plain and the surrounding regions (Abdelmaksoud et al. 2022, 2023; Ali et al. 2008; Bruno and Vesnaver 2021; Woodward 1994).

In addition, the borehole cross section (Fig. 3) reveals a thrust fault east of GWP-09, indicating the upward thrusting of pre-Asmari Formation rocks. Following the thrust fault, deposits of the Miocene Fars Formation and Oligocene Asmari Formation are absent in boreholes GWP-246A and GWP-247A. This thrust fault is also discernible in the interpreted seismic profiles (Figs. 4b and 5b). In the middle of the borehole cross section, two folds are apparent—a synclinal fold at positions GWP-010 and GWP-007, and an anticlinal fold at positions GPW-011 and GPW-006. Both of these folds have been reported in previous studies of the plain by Abdelmaksoud et al. (2023); Ali et al. (2008); Bruno and Vesnaver (2021); Woodward (1994). These two folds can also be observed in the interpreted seismic profiles (Figs. 4b and 5b). The existence of these three structural features—syncline, anticline, and thrust fault—on the borehole cross section (Fig. 3) and the interpreted seismic profiles is consistent with the information presented on the surface geological map (Fig. 1), which provides an overview of the surface and subsurface geological features.

The Bouguer anomaly map (Fig. 8a) provides insight into the lateral density variations with increasing values towards Jabal Mundassa on the northeast side of the study area. Jabal Mundassa is exposed to the Semail ophiolite, which was obducted during the Late Cretaceous period. Ali et al. (2008) interpreted the high positive residual gravity anomaly in the easternmost part of Al Jaww Plain as being related to the Semail ophiolite. The higher values in the map can be attributed to the presence of the ophiolite in the survey area, as ophiolites have higher density values compared to sedimentary rocks (Ali et al. 2020). The map delineates higher and lower Bouguer anomalies, approximately at the contour value of − 52 mGal, which can be interpreted as the contact of the Semail ophiolite in the survey area (Fig. 8a). The regional Bouguer anomaly exhibits a similar trend to the Bouguer anomaly (Fig. 8b).

The residual Bouguer anomaly map (Fig. 8c) reveals three zones within the survey area. A lower-density material zone is situated in the middle and is bounded by two higher-density zones. Field survey observations indicate that the higher residual anomaly zones in the northeast direction at Jabal Mundassa correspond to exposed Semail ophiolite rocks, whereas the higher residual Bouguer anomaly values on the southwest side may be attributed to a back thrust fault in the subsurface of the survey area. The residual Bouguer anomaly map also displays a small zone of low residual anomaly (< -0.80 mGal) in the north–south part of the survey area, which could be associated with an aquifer characterized by the accumulation of less dense sediment. The extent of the Semail ophiolite on Quaternary alluvium deposits, from the southeast to the northwest side near the -0.13 mGal contour value, is interpreted as the contact between the Semail ophiolite and sedimentary carbonate rocks (Fig. 8c).

The TMI map (Fig. 9a) indicates high values (>500 nT) on the northeast side, where the Semail ophiolite is exposed at Jabal Mundassa. An NW–SE-oriented feature with 75–150 m in thickness in the middle of the survey area exhibits the same TMI values as the features on the northeast side, suggesting that this feature could be a part of the Semail ophiolite that is not exposed on the surface. This feature is interpreted as a thin sheet of Semail ophiolite located at a distance from the exposed ophiolite at Jabal Mundassa (Fig. 9a). The RTP map enhances the NW–SE-oriented anomaly, which exhibits similar strength and characteristics to the eastern side, where the Semail ophiolite is exposed (Fig. 9b). The distance between the anomaly and the nearby exposed Semail ophiolite on the eastern side is approximately 500 m throughout the map (Fig. 9b). The anomaly closely corresponds to the Semail ophiolite contact interpreted from the residual Bouguer anomaly map (Fig. 8c).

The estimation of source body depths in potential field methods relies on the analysis of the power spectrum. Specifically, the radially averaged power spectrum is employed to determine the depths of both shallow and deep sources using gravity and magnetic data grids. This power spectrum, which depends on the wavenumber, is computed by averaging the energy across all directions for a given wavenumber (Grandis 2014). In the survey area, the radially averaged power spectrum of the Bouguer gravity data exhibits distinct features indicating both shallow and deep geological structures (Fig. 11). Shallow features are identified at an estimated depth of approximately 80 m, characterized by a gentle slope on the power spectrum window. Conversely, deep features exhibit a steeper slope on the power spectrum window, suggesting an approximate depth of 150 m. Based on the

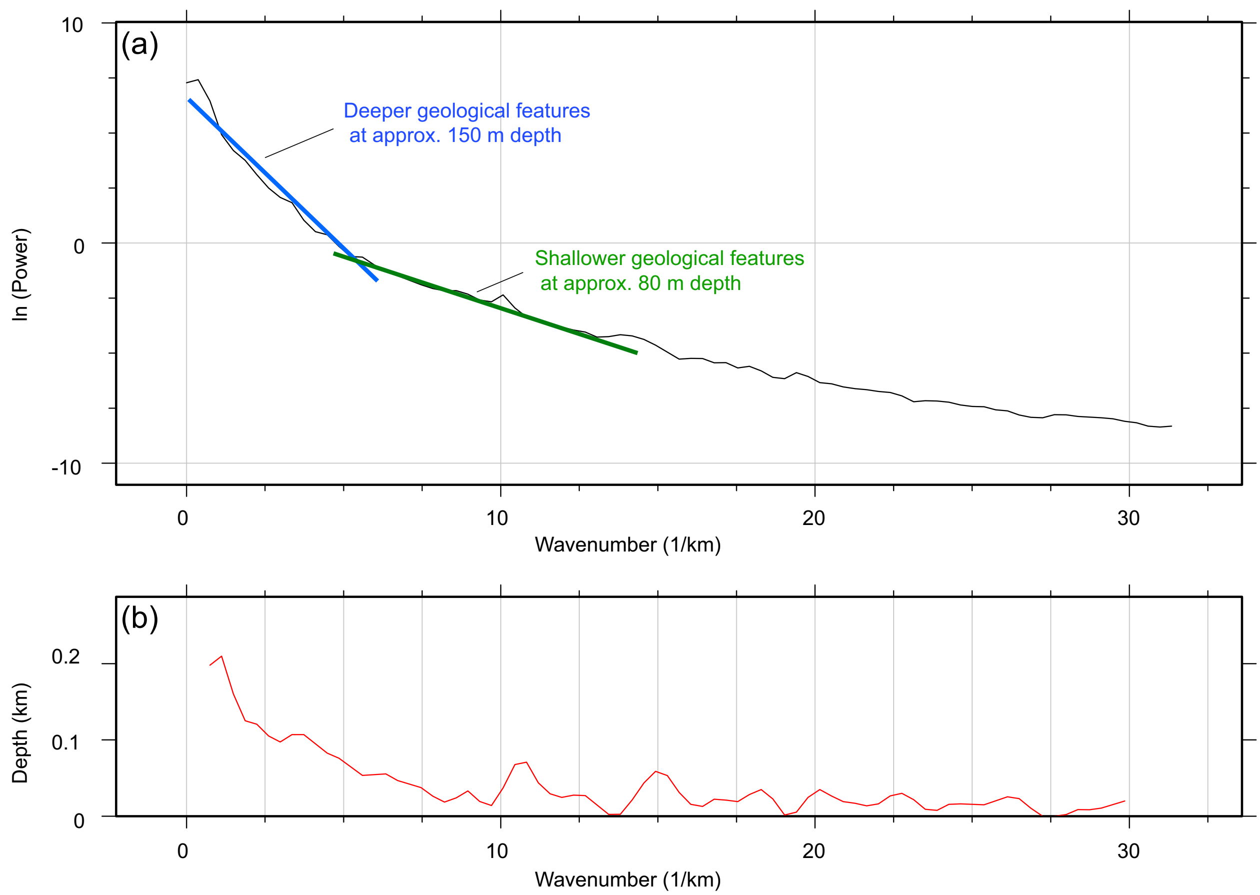

Fig. 11 **a** Radially average power spectrum and **b** depth estimate results of Bouguer anomaly of the survey area showing the shallow and deeper geological features

power spectrum analysis, the shallow geological features correspond to the Semail ophiolite, which is exposed in the northeast portion of the survey area, while the deeper geological features are indicative of allochthonous Hawasina thrust sheet or Cenozoic carbonate rocks in the western side (Fig. 11).

Furthermore, the radially averaged power spectrum applied to the TMI data provides insights into the depths of deep and shallow magnetic source bodies (Fig. 12). Deep magnetic sources exhibit high-angle slopes and lower wavenumbers on the power spectrum window, indicating an estimated depth of approximately 130 m. Conversely, shallow magnetic sources are characterized by low-angle slopes, suggesting an approximate depth of 70 m. The shallow source bodies identified in the radially averaged power spectrum can be attributed to the Semail ophiolite, given its high magnetic susceptibility values (Fig. 12). In addition, the NW–SE-oriented magnetic anomaly observed aligns with a shallow depth anomaly, corresponding to a depth of approximately 70 m from the surface (Figs. 11 and 12). The deep magnetic bodies, on the other hand, may originate from carbonate rocks and Hawasina thrust sheets, as their magnetic susceptibility values are lower compared to the Semail ophiolite.

Aquifers in Al Jaww Plain

Based on the borehole cross section (Fig. 3), the hydrogeological conditions in Al Jaww Plain indicate the presence of three interconnected groundwater aquifers, as summarized in Table 2. The first aquifer is the Quaternary unconfined aquifer, located in the near-surface alluvium deposits, which directly receives recharge from nearby mountains during the rainy season. This aquifer serves as the primary source of fresh groundwater in the southeastern part of Al Ain City (El-Mahmoudi et al. 2004). It consists of permeable sand and gravel deposits, with thickness ranging from 10 to 75 m, gradually increasing from the northeast to the southwest. On average, the Quaternary aquifer is approximately 25 m thick, although at borehole GWP-464, it reaches up to 75 m due to subsurface structural conditions. The hydraulic conductivity of this aquifer is relatively high due to its porous and

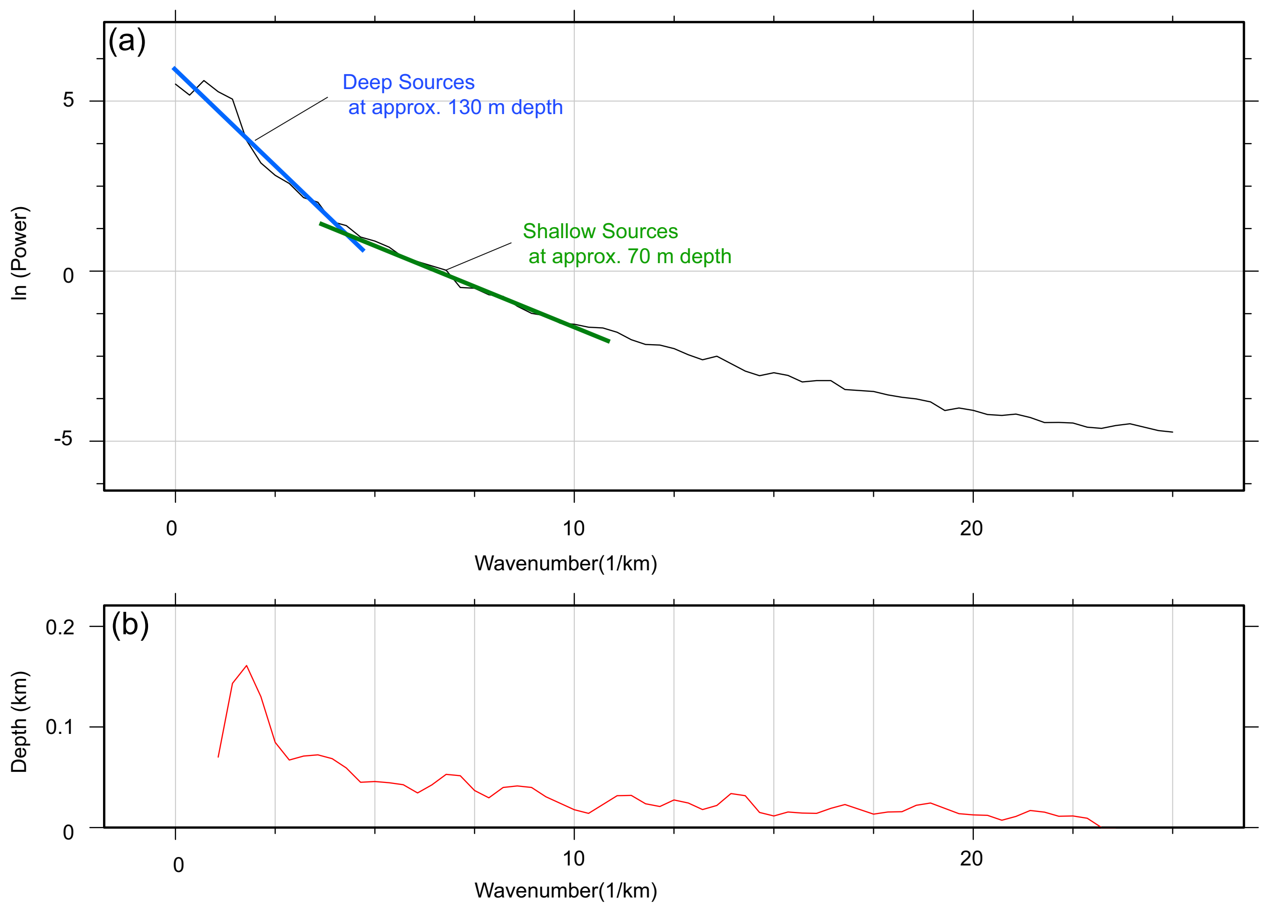

Fig. 12 **a** Radially average power spectrum and **b** depth estimate results of TMI of the survey area showing the shallow and deep sources

Table 2 Hydrogeological interpreted from groundwater borehole data in Al Jaww Plain

Hydrogeologic unit	Relative permeability (lithology)	Average aquifer thickness (m)	Aquifer type
Quaternary Alluvium	High-permeability (unconsolidated gravel and sand deposits)	25	Unconfined surficial system
Pliocene post-Fars Formation	Moderate permeability (gravel, silt, and calcareous sandstone)	110	Confined surficial system
Miocene Upper Fars Formation	Moderate permeability (mudstones and marls with limestone)	200	Confined surficial system
Miocene Lower Fars Formation	Low permeability (interbedded shales, mudstones, and evaporites)	> 200	Basal confining system

permeable nature, consistent with previous studies (Eggleston et al. 2020; El-Mahmoudi 2007).

The second aquifer is the Pliocene post-Fars aquifer, which is interconnected with the upper Quaternary freshwater aquifer. It comprises interbedded gravel, silt, calcareous sandstone, and clay. The thickness of the post-Fars aquifer varies from 40 to 200 m, with greater thickness observed in the southwest part of the borehole cross section, where a syncline fold is present at borehole GWP-010. On average, this aquifer is approximately 110 m thick and is considered part of the surficial aquifer system. However, it is not reported in the eastern part of the plain beyond the thrust fault. The Quaternary and Pliocene post-Fars aquifers are regarded as a single major aquifer unit with an average thickness of 60 m in Al Jaww Plain.

The third aquifer in Al Jaww Plain belongs to the Upper Fars Formation and is interconnected with the second Pliocene post-Fars aquifer. It consists of intercalated marine to terrestrial mudstones, marl, and limestone. This aquifer has an average thickness of approximately 200 m and is predominantly located in the southwestern part of the borehole cross section, near Jabal Hafit. It is absent in the eastern part of the plain. Due to the mudstone nature of the rocks, the permeability of this aquifer is moderate to low, and it exhibits higher salinity content (Al Nuaimi 2003). The Miocene Lower Fars Formation, composed of marine sequence rocks, has very low permeability due to its lithological properties and does not qualify as an aquifer. It is interpreted as a basal confining system within the hydrologic unit of Al Jaww Plain (Al Nuaimi 2003).

The hydrogeological characteristics identified in the survey area align with the properties of the unconfined Quaternary aquifers reported in Table 2. Moreover, the interpretation of the ERT inverted sections is based on data from borehole GWP-251, located approximately 2.3 km south of the survey area (Fig. 1). The lithological description of borehole GWP-251 indicates that the lithology from the surface to a depth of 24 m consists of gravel, sand, and clay. From 24 to 100 m depth, the rock units are characterized by interbedded claystone and limestone formations.

A prominent high resistivity layer with values exceeding 115 Ωm was observed near the surface along all ERT inverted sections (Fig. 10). This zone corresponds to unsaturated sand and gravel material. The approximate thickness of the near-surface high resistive layer is 15 m along Lines 1 and 2, while it decreases to approximately 10 m along Line 5 (Fig. 10). The water table is interpreted to be at a depth approximately equal to the thickness of the first layer. Notably, Line 6 demonstrates variable resistivity values near the surface. This line was acquired on an exposed ophiolite surface, oriented from south to north. The surface position between 220 and 340 m exhibits very high resistivity values exceeding 250 Ωm, which corresponds to the location of the exposed unsaturated ophiolite. A moderately resistive section is observed beneath this zone, which extends to a depth of approximately 50 m. This portion is interpreted as the saturated zone of the ophiolite.

The second layer, characterized by moderate resistivity values ranging from 15 to 115 Ωm, is interpreted as saturated sand and gravel deposits. This layer is identified as part of the unconfined Quaternary aquifer in Al Jaww Plain, as its resistivity values align with those of fresh groundwater. Its approximate thickness is 20–25 m, with slight variations observed across the ERT sections. The water table acts as a boundary between the first and second layers, delineated by a change in resistivity values within the same type of material. The aquifer receives direct recharge from small water channels originating from nearby Jabal Mundassa during the rainy season.

The third layer exhibits very low resistivity values (< 10 Ωm) and consists of marl, clay, and mudstone materials, rendering it conductive. This layer sometimes intermixes with the lower part of the second layer due to variations in lithological units. These variations are clearly visible through changes in resistivity values across all the ERT sections. The presence of very low resistivity values (< 5 Ωm) within the third layer can likely be attributed to an increase in salinity content within the mudstone layer (Fig. 10).

It is worth noting that determining precise uncertainties for our estimated values is challenging. However, it is important to note that there are inherent uncertainties in our hydrogeological property estimates. These uncertainties arise from a combination of factors, including the limited availability of groundwater borehole data, reliance on existing literature, and interpretation of geophysical data. In addition, boreholes, such as MD-1 and groundwater boreholes, did not penetrate all strata, such as the Hawasna thrust, which introduces uncertainty regarding the thickness of specific units.

Conclusions

The integrated geophysical groundwater borehole findings in this study provide comprehensive insights into the shallow and deep characteristics of groundwater aquifers, ophiolite contact, and tectonic structures in Al Jaww Plain. Analysis of groundwater borehole data reveals the existence of three interconnected types of aquifers with distinct hydrogeological properties. The Quaternary unconfined aquifer, predominantly composed of sand and gravel deposits in the near-surface alluvium, exhibits an average thickness of approximately 25 m and demonstrates higher hydraulic conductivity due to its porous and permeable nature. The second aquifer, associated with the upper Quaternary freshwater aquifer, consists of gravel, silt, calcareous sandstone, and interbedded clay rocks, with a thickness ranging from 40 to 200 m, peaking on the southwest side of the plain. This aquifer, with an average thickness of about 110 m, is considered part of the surficial aquifer system. The third aquifer, attributed to the Upper Fars Formation, comprises intercalated marine to terrestrial mudstones, marls, and limestone, with an average thickness of approximately 200 m, predominantly located in the southwest region of the plain. This aquifer demonstrates moderate to low permeability and higher salinity. The Miocene Lower Far Formation, consisting of marine sequence rocks, acts as a basal confining system. The relative porosity and permeability of the aquifers vary from high to low with increasing depth in Al Jaww Plain.

The inversion results of ERT data aid in elucidating the hydro-stratigraphic properties of the near-surface Quaternary aquifer within the survey area. The ERT inverted sections consistently depict lateral and vertical variations in true resistivity, representing a three-layer scenario. The estimated water table lies at a depth of 10–15 m below the surface in all ERT sections. A freshwater unconfined aquifer is identified within the saturated sand and gravel deposits, replenished directly by water channels originating from Jabal Mundassa. The average thickness of the Quaternary alluvium, approximately 30 m, corresponds to the properties of the shallow unconfined aquifer throughout Al Jaww Plain.

Within the southeastern survey area of Al Jaww Plain, the Bouguer anomaly map delineates higher and lower Bouguer anomalies, indicative of the Semail ophiolite contact. The residual Bouguer anomalies map reveals three distinct zones within the survey area. A lower-density zone occupies the middle region, bounded by two higher-density zones, while a very low-density area in the north–south direction of the survey area exhibits potential for groundwater extraction. The thrusting of the Semail ophiolite over the Quaternary alluvium deposits on the northeast side corresponds to the contact between the Semail ophiolite and sedimentary carbonate rocks. The power spectrum analysis of gravity and magnetic data indicates the approximate depths of shallow to deep geological features and source bodies at 70–80 m and 130–150 m, respectively, within the survey area.

An NW–SE-oriented linear feature observed in the middle of the magnetic maps within the survey area is interpreted as a thin (75–150 m) mantle thrust sheet beneath the surface, which becomes apparent at a distance from the Semail ophiolite exposure at Jabal Mundassa. The location of the magnetic anomaly aligns with the interpretation of the Semail ophiolite contact on the residual Bouguer gravity map, thus confirming the ophiolite contact location.

Acknowledgements
We are thankful to Khalifa University of Science and Technology for the sponsorship of this study during the student's field trip. We are grateful to ADNOC for the permission to publish the seismic profiles and to Environment Agency Abu Dhabi for providing the groundwater borehole data. The authors also thank the teaching faculty and undergraduate students of the Earth Science Department of Khalifa University for their support during gravity, magnetic, and ERT surveys. Geosoft was used to grid and plot the gravity and magnetic data, and Res2DInv version 4.10 was used to process and invert the ERT data.

Author contributions
SU, MA, MI, and FB performed the field survey. SU and MA contributed to the interpretation of the results and the preparation of the manuscript. All authors read and approved the final manuscript.

Funding
This research is supported by Khalifa University of Science and Technology (KUST).

Availability of data and materials
The data are available upon request to the authors.

Declarations

Competing interests
The authors declare that they have no competing interests.

Received: 13 July 2023 Accepted: 4 November 2023
Published online: 19 November 2023

References
Abd-Allah AM, Hashem WA, Abdelghany O (2013) Structural and tectonostratigraphic evolution of the Upper Cretaceous-Eocene sequence in Malaqet–Mundassah–El Saah Range, Oman Mountains, United Arab Emirates and Oman. J Afr Earth Sc 79:111–124
Abdelghany O (2003) Late Campanian-Maastrichtian foraminifera from the Simsima Formation on the western side of the Northern Oman Mountains. Cretac Res 24(4):391–405
Abdelmaksoud A, Ali M, Searle M (2022) Tectono-stratigraphic evolution of the foreland fold-and-thrust belt of the United Arab Emirates. Tectonics 41(9):e2022TC007470
Abdelmaksoud A, Ali MY, Geng M, Saibi H (2023) Basement morphology of the fold-and-thrust belt and foreland basin of the United Arab Emirates: evidence for thick-skinned tectonics in the northern Oman-UAE Mountains. Tectonophysics 856:229838
Abdelrazek M (2020) Applications of Geophysical Methods "Geophysics and Oil Exploration". Ain Shams Engineering Journal 1.54 MB:11
Al Nuaimi H (2003) Hydrogeological and Geophysical Studies on Al Jaww plain, Al Ain Area, United Arab Emirates. Sc Thesis United Arab Emirates University, Al Ain 159
Ali MY, Sirat M, Small J (2008) Geophysical investigation of Al Jaww Plain, eastern Abu Dhabi: Implications for structure and evolution of the frontal fold belts of the Oman Mountains. GeoArabia 13(2):91–118
Ali M, Sirat M, Small J (2009) Integrated gravity and seismic investigation over the Jabal Hafit structure: Implications for basement configuration of the frontal fold-and-thrust belt of the northern Oman Mountains. J Pet Geol 32(1):21–37
Ali M, Watts A, Searle M, Keats B, Pilia S, Ambrose T (2020) Geophysical imaging of ophiolite structure in the United Arab Emirates. Nat Commun. https://doi.org/10.1038/s41467-020-16521-0
Binley A, Hubbard SS, Huisman JA, Revil A, Robinson DA, Singha K, Slater LD (2015) The emergence of hydrogeophysics for improved understanding of subsurface processes over multiple scales. Water Resour Res 51(6):3837–3866
Boote D, Mou D, Waite R (1990) Structural evolution of the Suneinah foreland, central Oman Mountains. Geo Soc London Spec Publicat 49(1):397–418
Bruno PPG, Vesnaver A (2021) Groundwater characterization in arid regions using seismic and gravity attributes Al Jaww Plain UAE. Front Earth Sci. https://doi.org/10.3389/feart.2020.575019
Casallas-Moreno K, González-Escobar M, Gómez-Arias E, Mastache-Román E, Gallegos-Castillo C, González-Fernández A (2021) Analysis of subsurface structures based on seismic and gravimetric exploration methods in the Las Tres Vírgenes volcanic complex and geothermal field, Baja California Sur. Mexico Geothermics 92:102026
Cooper D, Ali M, Searle M (2014) Structure of the northern Oman Mountains from the Semail Ophiolite to the Foreland Basin. Geo Soc London Spec Publicat 392(1):129–153
Dunne L, Manoogian P, Pierini D (1990) Structural style and domains of the northern Oman Mountains (Oman and United Arab Emirates). Geo Soc London Spec Publicat 49(1):375–386
Eggleston JR, Mack TJ, Imes JL, Kress W, Woodward DW, Bright DJ (2020) Hydrogeologic framework and simulation of predevelopment groundwater flow, eastern Abu Dhabi Emirate, United Arab Emirates. Scientific Investigations Report. Reston, VA. Doi: https://doi.org/10.3133/sir20185158

El-Mahmoudi AS (2007) The Application of two-dimensional electrical resistivity imaging for mapping the quaternary aquifer at Wadi Muraykhat and Wadi Sa'a, Al Ain area UAE. J Appl Geophys 6(2):13–28
El-Mahmoudi A, Al-Nuaimi H, Sherif M (2004) Geophysical and hydrogeological investigations of the quaternary aquifer at Al Jaww Plain, Al Ain area. UAE Fast times 9(1):17–28
Glennie KW (1974) Geology of the Oman mountains. Verhandelingen van het Koninklink Nederlands Geologisch Mijnbouwkundig Genootchachp 1:423
Grandis H (2014) Simulation of 3D gravity anomaly of thin coal layer in sedimentary environment and its delineation. Int J Tomograp Simulat 26(2):1–11
Kane M (1962) A comprehensive system of terrain corrections using a digital computer. Geophysics 27(4):455–462
Kress W (2017) Hydrogeologic characterization of the surficial aquifer system, and the influence of shallow structural features on movement and quality of water, northeast Abu Dhabi Emirate, UAE The Petroleum Institute, Abu Dhabi, UAE,
Loke MH, Dahlin T (2002) A comparison of the Gauss-Newton and quasi-Newton methods in resistivity imaging inversion. J Appl Geophys 49(3):149–162
Loke MH (2004) Tutorial: 2-D and 3-D electrical imaging surveys.
Luo Y, Xue DJ, Wang M (2010) Reduction to the pole at the geomagnetic equator. Chinese J Geophy 53(6):1082–1089
Menges C, Hadley D, Woodward D, Mohamed F (1993) Geology and geophysics, groundwater resources of Al-Ain area, Abu Dhabi Emirate. US Geo Survey Administrat Rep 93:74–167
Nagy D (1966) The gravitational attraction of a right rectangular prism. Geophysics 31(2):362–371
Noweir MA (2000) Back-thrust origin of the Hafit structure, northern Oman Mountain front United Arab Emirates. Geoarabia 5(2):215–228
Rabeh T, Ali K, Bedair S, Sadik MA, Ismail A (2019) Exploration and evaluation of potential groundwater aquifers and subsurface structures at Beni Suef area in southern Egypt. J Afr Earth Sc 151:9–17
Rabu D, Nehlig P, Roger J (1993) Stratigraphy and structure of the Oman Mountains. Documents-B R G M
Searle M (1988) Thrust tectonics of the Dibba zone and the structural evolution of the Arabian continental margin along the Musandam Mountains (Oman and United Arab Emirates). J Geol Soc 145(1):43–53
Searle MP (2007) Structural geometry, style and timing of deformation in the Hawasina Window, Al Jabal al Akhdar and Saih Hatat culminations. Oman Mountains Geoarabia 12(2):99–130
Searle MP, Ali MY (2009) Structural and tectonic evolution of the Jabal Sumeini–Al Ain-Buraimi region, northern Oman and eastern United Arab Emirates. GeoArabia 14(1):115–142
Searle M, Cox J (1999) Tectonic setting, origin, and obduction of the Oman ophiolite. Geol Soc Am Bull 111(1):104–122
Searle M, Cooper D, Watts K (1990) Structure of the Jebel Sumeini-Jebel Ghawil area, Northern Oman. Geo Soc London Spec Publicat 49(1):361–374
Styles M, Ellison R, Arkley S, Crowley QG, Farrant A, Goodenough KM, McKervey J, Pharaoh T, Phillips E, Schofield D (2006) The geology and geophysics of the United Arab Emirates: Volume 2, geology.
Warburton J, Burnhill T, Graham R, Isaac K (1990) The evolution of the Oman Mountains foreland basin. Geo Soc London Spec Publicat 49(1):419–427
Wilson HH (2000) The age of the Hawasina and other problems of Oman Mountain geology. J Pet Geol 23(3):345–362
Woodward D (1994) Contributions to a shallow aquifer study by reprocessed seismic sections from petroleum exploration surveys, eastern Abu Dhabi, United Arab Emirates. J Appl Geophys 31(1–4):271–289

Publisher's Note

Springer Nature remains neutral with regard to jurisdictional claims in published maps and institutional affiliations.